Membrane Permeabilization Mechanisms of a Cyclic Antimicrobial Peptide, Tachyplesin I, and Its Linear Analog†

Katsumi Matsuzaki,*,‡ Shuji Yoneyama,‡ Nobutaka Fujii,‡ Koichiro Miyajima,‡ Ken-ichi Yamada,§ Yutaka Kirino,|| and Kazunori Anzai*,⊥

Faculty of Pharmaceutical Sciences, Kyoto University, Sakyo-ku, Kyoto 606-01, Japan, Faculty of Pharmaceutical Sciences, Kyushu University, Higashi-ku, Fukuoka 812, Japan, Faculty of Pharmaceutical Sciences, The University of Tokyo, Bunkyo-ku, Tokyo 113, Japan, and National Institute of Radiological Sciences, Inage-ku, Chiba 263, Japan

Received March 14, 1997; Revised Manuscript Received May 9, 1997⊗

ABSTRACT: Tachyplesin I (T-SS), an antimicrobial peptide from *Tachypleus tridentatus*, has a cyclic antiparallel β-sheet structure maintained by two disulfide bridges. The peptide effectively permeabilizes both bacterial and artificial lipid membranes. T-Acm, a linear analog peptide with the four SH groups protected by acetamidomethyl groups, exhibits a much weaker membrane-permeabilizing activity in spite of a greater disruption of the lipid organization [Matsuzaki, K., Nakayama, M., Fukui, M., Otaka, A., Funakoshi, S., Fujii, N., Bessho, K., & Miyajima, K. (1993) *Biochemistry 32*, 11704−11710]. To clarify the efficient permeabilization mechanism of T-SS, we studied the interactions of both peptides with liposomes and planar lipid bilayers. The cyclic peptide capable of spanning the bilayer (ca. 3 nm length) was found to form an anion-selective pore and translocate across the bilayer coupled with the pore formation. A *cis*-negative transmembrane potential facilitated the pore formation compared with the *cis*-positive potential. In contrast, the linear peptide failed to translocate. Instead, it impaired the membrane barrier by disrupting the lipid organization with morphological changes in the vesicles.

Tachyplesin I (T-SS;[1] Figure 1) is an antimicrobial peptide isolated from the acid extracts of hemocytes of the horseshoe crab, *Tachypleus tridentatus* (Nakamura et al., 1988). The heptadecapeptide is considered to exert its bactericidal activity by permeabilizing bacterial membranes, although the molecular mechanism has not yet been determined (Matsuzaki et al., 1991; Ohta et al., 1992). T-SS forms a cyclic antiparallel β-sheet structure because of its two disulfide bonds (Kawano et al., 1990; Tamamura et al., 1993b). To elucidate the role of the SS linkages, we synthesized a linear analog (T-Acm; Figure 1) and compared its activity with that of the parent T-SS (Matsuzaki et al., 1993b; Tamamura et al., 1993a). T-Acm was found to be weaker than T-SS in both its antibacterial potency and lipid bilayer-permeabilizing ability, the latter being evaluated by the efflux of a water-soluble fluorescent dye, calcein, from liposomes. Interestingly, however, the weaker, linear peptide more strongly perturbed the bilayer organization as revealed by an FTIR-PATR technique. Therefore, we speculated that T-SS provides an effective membrane-permeabilizing mechanism different from that of T-Acm, the latter appearing to be the membrane disintegration.

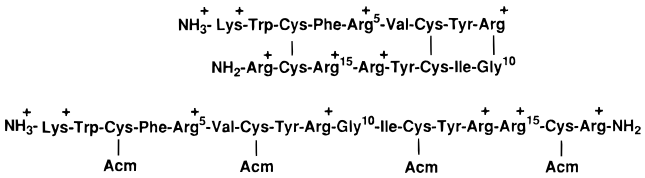

FIGURE 1: Amino acid sequences of T-SS (top) and T-Acm (bottom).

One possibility is that T-SS forms an ion channel or a channel-like pore. The size of T-SS (ca. 3 nm long) allows the amphiphilic peptide to span the bilayer. However, such a scheme is apparently incompatible with the observation that the β-sheet lies parallel to the membrane surface as determined by the FTIR−PATR method (Matsuzaki et al., 1993b). We have encountered similar phenomena in studying amphiphilic helical peptides, magainin 2 (Matsuzaki et al., 1994, 1995a,b) and mastoparan X (Matsuzaki et al., 1996b). Both peptides construct calcein-permeable pores whose lifetimes are relatively short. A couple of studies using solid state NMR (Bechinger et al., 1991) and fluorescence quenching (Matsuzaki et al., 1994) clarified that the magainin helix essentially lies parallel to the membrane surface. The parallel orientation was also deduced for the mastoparan X helix from fluorescence quenching of an anthryl-modified peptide by spin-labeled lipids (Fujita et al., 1994). We have elucidated that these helical peptides

† Supported by the Naito Foundation, the Research Foundation for Pharmaceutical Sciences, and Grant-in-Aids for Scientific Research on Priority Areas (No. 08219223) and for Encouragement of Young Scientists (No. 09771946) from the Ministry of Education, Science and Culture of Japan.

* Authors to whom correspondence should be addressed.
‡ Kyoto University.
§ Kyushu University.
|| The University of Tokyo.
⊥ National Institute of Radiological Sciences.

⊗ Abstract published in *Advance ACS Abstracts,* July 15, 1997.

[1] Abbreviations: T-SS, tachyplesin I; T-Acm, an acyclic tachyplesin I analog with the four SH groups of tachyplesin I protected by acetamidomethyl groups; PC, egg yolk L-α-phosphatidylcholine; PG, L-α-phosphatidylglycerol enzymatically converted from PC; PE, egg yolk L-α-phosphatidylethanolamine; DNS-PE, *N*-[[5-(dimethylamino)-naphthyl]-1-sulfonyl]dipalmitoyl-L-α-phosphatidylethanolamine; LUVs, large unilamellar vesicles; MLVs, multilamellar vesicles; RET, resonance energy transfer; FTIR−PATR, Fourier transform infrared−polarized attenuated total reflection; L/P, lipid-to-peptide molar ratio; NBD, 7-nitrobenz-2-oxa-1,3-diazol-4-yl.

S0006-2960(97)00588-6 CCC: $14.00

translocate across the bilayers upon the disintegration of the unstable pores. Few pores exist after the redistribution of the peptides between the two leaflets, because the pore formation is a highly cooperative process. Therefore, spectroscopic measurements in the equilibrium state fail to detect the pore structure; the peptides lie parallel to the membrane surface instead of spanning the bilayer.

In this paper, we examined the translocation of T-SS and T-Acm across PG/PC bilayers, i.e., the movement of the peptides from the outer to the inner leaflets, and found that only T-SS has the potency of translocating the membrane. On the other hand, T-Acm permeabilized the bilayer via morphological changes of the liposomes. However, the results depended on the lipid composition. PG/PE liposomes mimicking bacterial plasma membranes were found to be more resistant to T-SS, whereas they were more susceptible to T-Acm. To get an insight into the pore structure, we also determined the ion channel activity of T-SS and T-Acm in planar lipid bilayers. The cyclic peptide formed an anion-selective channel, whereas the linear peptide failed to induce any current. The differences between the two peptides were discussed in terms of the peptide structures.

MATERIALS AND METHODS

Materials. T-SS and T-Acm were synthesized by Fmoc-based solid phase synthesis and authenticated as described elsewhere (Akaji et al., 1989). The synthesized peptides were initially purified by RP-HPLC and then further refined by gel filtration (Sephadex G-15, 2.5 × 35 cm column, 0.02 M HCl being used as an eluent), followed by lyophilization. The purities (ca. 100%) were determined by quantitative amino acid analysis. The concentration of the peptides was routinely measured by their optical density at 280 nm.

PC was purchased from Sigma (St. Louis, MO). PG, which was enzymatically converted from PC, was either a gift from Nippon Fine Chemical Co. (Takasago, Japan) or a product of Sigma. PE was obtained from Avanti (Alabaster, AL) or Sigma. DNS-PE was a product of Molecular Probes (Eugene, OR). Calcein and spectrograde organic solvents were provided by Dojindo Laboratory (Kumamoto, Japan). All other chemicals from Wako (Tokyo, Japan) were of special grade. A Tris buffer (10 mM Tris-HCl/150 mM NaCl/1 mM EDTA, pH 7.0) was prepared with water twice distilled from a glass still.

Vesicle Preparation. LUVs were prepared by the extrusion of MLVs, as described elsewhere (Matsuzaki et al., 1994). Briefly, a lipid film, after being dried under vacuum overnight, was hydrated with a 70 mM calcein solution for the dye release assay (pH was adjusted to 7.0 with NaOH) or the Tris buffer for the other experiments and vortex mixed to produce the MLVs. The suspension was freeze−thawed for five cycles and then successively extruded through polycarbonate filters (a 0.6 μm pore size filter, 5 times; two stacked 0.1 μm pore size filters, 10 times). The lipid concentration was determined in triplicate by phosphorus analysis (Bartlett, 1959).

Leakage. The calcein-entrapped LUVs were separated from free calcein on a Biogel A-1.5m column and mixed with the calcein-free vesicles. The release of calcein from LUVs was fluorometrically monitored at an excitation wavelength of 490 nm and an emission wavelength of 520 nm on a Shimadzu RF-5000 spectrofluorometer whose cuvette holder was thermostated at 30 ± 0.5 °C. The apparent percent leakage value at a fluorescence intensity, F, was calculated by eq 1:

$$\%\ \text{leakage (apparent)} = 100 \times (F - F_0)/(F_t - F_0) \quad (1)$$

F_t denotes the fluorescence intensity corresponding to 100% leakage after the addition of 10% Triton X-100 (20 μL) to 2 mL of the sample. F_0 represents the fluorescence of the intact vesicle. The apparent percent leakage value was converted to the true one as described in the Discussion. The reported time courses of the leakage were the average of 2−3 experiments.

90° Light Scattering. Changes in vesicle size were followed by measuring the light scattering intensity at the right angle. Both the excitation and emission wavelengths of the spectrofluorometer were set at 400 nm. The intensity of the peptide-treated liposomes was expressed relative to the value of the control vesicles without the peptide.

Resonance Energy Transfer (RET). Symmetrically labeled LUVs were prepared by hydrating the lipid film composed of PC, PG, and DNS-PE in a molar ratio of 5:4:1. RET from the Trp residue of the peptide to the dansyl chromophore in the membrane was monitored by observing the fluorescence intensity of the Trp residue (336 nm) upon excitation at 280 nm. The temperature was controlled at 30 ± 0.5 °C.

Formation of Planar Bilayer Membrane. Planar lipid bilayers were formed by the folding method (Takagi et al., 1965; Montal & Mueller, 1972). This procedure uses a Teflon chamber with two compartments (each about 1.5 mL in internal volume) separated by a Teflon septum (25 μm thick) with a 200 μm diameter aperture. A small amount (15−20 μL) of a lipid solution in *n*-hexane (10 mg/mL) was placed on the surface of an electrolyte solution (0.5 mL in each compartment) in the chamber. A lipid monolayer was spontaneously formed at the air/water interface after the evaporation of the solvent in a few minutes. The water level in each compartment was then raised over the aperture, where the lipid bilayer subsequently formed.

Measurement of Membrane Current. A small amount of a peptide solution in a buffer (100 mM KCl/10 mM Tris-Hepes, pH 7.4) was added to one compartment of the chamber, which was defined as the *cis* compartment. The *cis* solution was continuously stirred with a magnetic stirrer under an applied membrane potential until a current fluctuation occurred. The potential was expressed as that of the *cis* compartment relative to the *trans* side, which is held at virtual ground. The current across the membrane was measured with a handmade current/voltage converter (bandwidth 800 Hz) and was displayed on both a digital storage oscilloscope (COR5521, Kikusui Electronics, Kawasaki, Japan) and a chart recorder (R61VL, Rikadenki, Tokyo, Japan). The data were accumulated by use of a videotape recorder (SL-HF3, Sony, Tokyo, Japan) after A/D conversion with a modified digital audio processor (PCM-501ES, Sony) (Fujiwara et al., 1988). Selected parts of the recorded data were transcribed on a thermal arraycorder (WR7400, Graphtec, Tokyo, Japan; frequency response, 200 Hz).

The Goldman−Hodgkin−Katz equation was used to evaluate the ion selectivity from the reversal potential of the macroscopic current, $\Delta\Psi_{rev}$, measured in asymmetric KCl solutions containing 10 mM Tris-Hepes (pH 7.4) after a

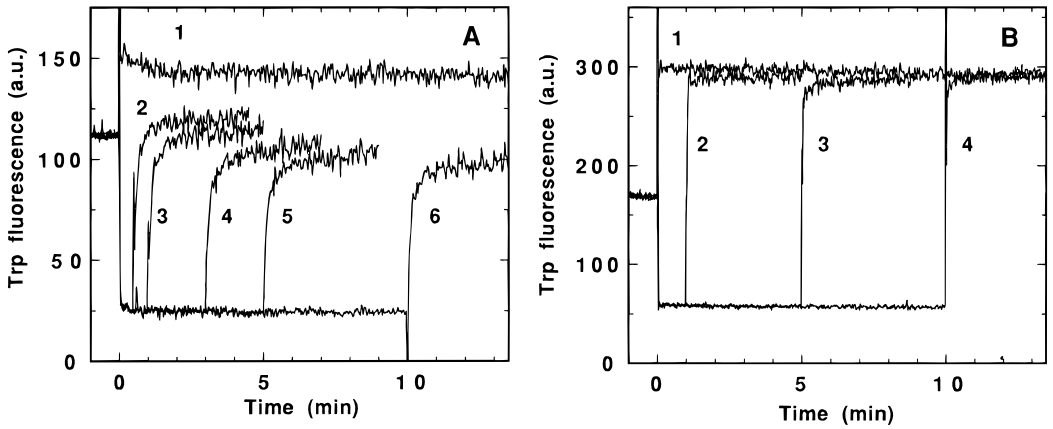

FIGURE 2: Detection of the peptide translocation. T-SS (A) or T-Acm (B) was mixed with dansyl LUVs (PG/DNS-PE/PC = 4/1/5) at time zero. The final peptide concentration was 2 μM. The lipid concentration was 232 μM (A) or 200 μM (B). The fluorescence intensity of Trp at 336 nm (excited at 280 nm) was recorded. The binding of the peptide to the vesicle reduced the intensity due to RET. At various time intervals of incubation [0.5, 1, 3, 5, and 10 min, traces 2−6 (A); or 1, 5, and 10 min, traces 2−4 (B)], a large excess (final concentration 938 μM) of the second population of dansyl-free LUVs (PG/PC = 1/1) was added. An increase in intensity indicates the relief from RET caused by the redistribution between the two vesicle populations of the peptide molecules which had been bound to the outer surface of the first vesicle. In the case of T-SS (A), the increased intensity decreases with prolonged incubation and is smaller than the fluorescence intensity when both populations of vesicles were simultaneously added at time zero (trace 1), thus indicating that some of the peptides translocated into the inner leaflet during the incubation. In contrast, no translocation was observed for T-Acm (B). Each trace is the average of three experiments.

correction for the liquid junction potential:

$$\frac{P_{Cl}}{P_K} = \frac{[C_K^{trans} - C_K^{cis}\exp(F\Delta\Psi_{rev}/RT)][1 - \exp(-F\Delta\Psi_{rev}/RT)]}{[C_{Cl}^{trans} - C_{Cl}^{cis}\exp(-F\Delta\Psi_{rev}/RT)][1 - \exp(F\Delta\Psi_{rev}/RT)]} \quad (2)$$

The electrolyte concentration in each compartment is denoted by *C*. The Faraday and the gas constants are represented by *F* and *R*, respectively. The absolute temperature is expressed as *T*.

RESULTS

Translocation and Pore Formation of T-SS in PG/PC Bilayers. The translocation was detected by the measurement of the amount of the untranslocated peptides remaining in the outer monolayers (Matsuzaki et al., 1995a). The untranslocated peptides can be readily removed from the vesicle surface by extraction with a large excess of a second population of vesicles.[2] The unremovable fraction was determined by use of RET from the Trp residue of the peptide to the dansyl chromophore (DNS-PE) incorporated into the membrane phase. Figure 2A exhibits the data for T-SS at L/P = 116 where a significant membrane permeabilization occurs (see Figure 3). The addition of dansyl-labeled vesicles (232 μM) to a peptide solution (2 μM) at time zero resulted in a significant decrease in Trp fluorescence, indicating RET due to the binding of the peptide to the membrane.[3] After a short incubation for 0.5 min, a second population of dansyl-free vesicles (938 μM, DNS-PE was substituted by PG) was added in large excess (trace 2). An abrupt increase in the fluorescence intensity implies that the peptide molecules, which had been bound to the *outer* leaflet, were redistributed between the two vesicle populations, resulting in relief from RET.[4] The increased fluorescence intensity was, however, smaller than the intensity when both vesicle populations were simultaneously added to the peptide solution at time zero (trace 1), suggesting that a fraction of the peptides became unexposed to the outer surface and therefore untransferable to the second vesicles. The buried

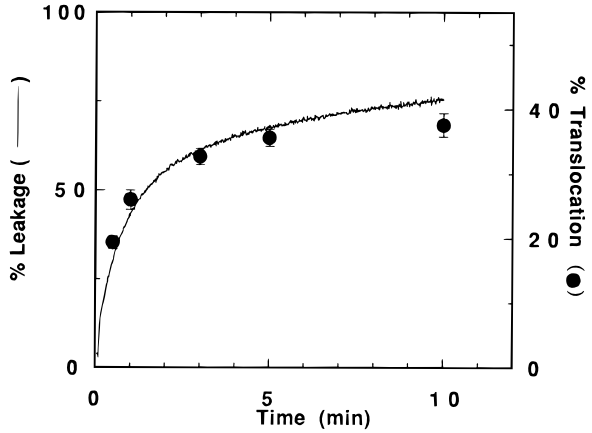

FIGURE 3: Coupling between pore formation and peptide translocation for T-SS. The pore formation was estimated on the basis of the leakage of calcein from PG/PC (1/1) LUVs. The peptide and lipid concentrations were the same as those of Figure 2. The translocation was evaluated by the method in Figure 2A.

[2] In these studies, we used liposomes containing 50 mol % acidic phospholipids, whereas 100% PG was used in our previous study (Matsuzaki et al., 1993b). The incorporation of more than 50 mol % acidic lipids inhibited the rapid removal of the untranslocated peptides with the vesicles because of the excessively strong binding.

[3] DNS-PE (10 mol %) quenches 86% of the Trp fluorescence (Matsuzaki et al., 1996b). If the peptide molecules are completely bound to the membrane, that is, the reduced fluorescence totally originates from the peptide bound to the dansyl vesicles, the fluorescence intensity (trace 1) after the simultaneous addition of the dansyl vesicles (232 μM) and the dansyl-free vesicles (938 μM) should be larger by a factor of [(1 − 0.198) + 0.198 × 0.14]/0.14 = 5.9 (0.198: the traction of the dansyl vesicles). This factor is exactly the same as found (Figure 2A), indicating the complete binding of the peptide.

[4] The slower phase of the fluorescence recovery is probably due to the back-translocation (outward movement of the translocated peptide).

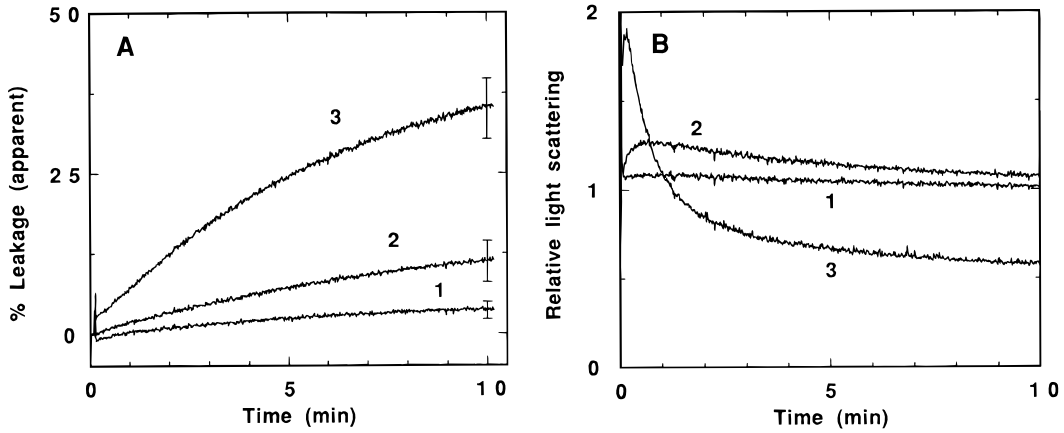

FIGURE 4: Membrane permeabilization (A) and morphological changes (B) of PG/PC (1/1) LUVs induced by T-Acm. (A) The percent leakage of calcein was plotted as a function of time. L/P: trace 1, 10; 2, 5; 3, 2.6. (B) The 90° light scattering intensity at 400 nm was represented as the value relative to the control value without the peptide. L/P: trace 1, 52; 2, 21; 3, 10.

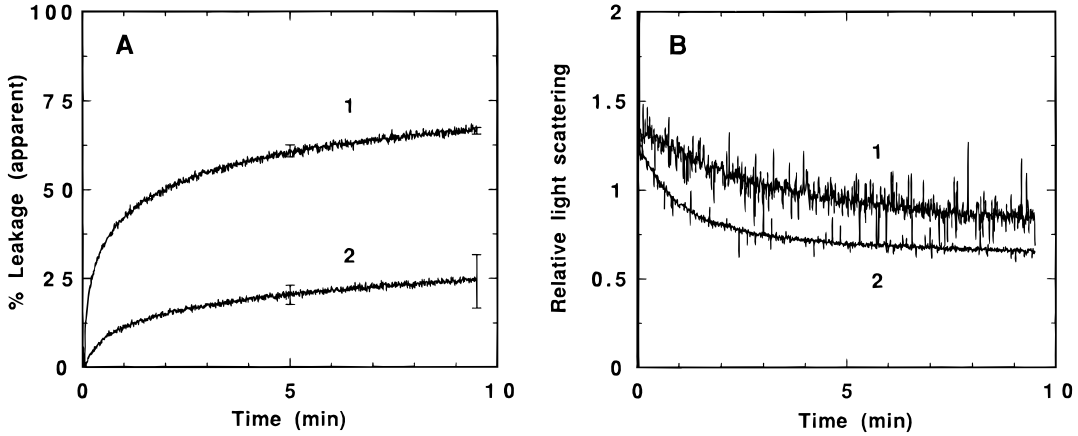

FIGURE 5: Membrane permeabilization (A) and morphological changes (B) of PG/PE (1/1) LUVs induced by T-SS and T-Acm. The percent leakage of calcein (A) and the relative 90° light scattering intensity at 400 nm (B) were plotted as a function of time. Trace 1: T-SS, L/P = 27. Trace 2: T-Acm, L/P = 8.5.

fraction increased with the incubation time (traces 2−6), indicating a time-dependent peptide internalization.

Figure 3 compares the translocation (closed circles) with the pore formation (trace) at the same L/P value of 116. To estimate the percent translocation value, we used the fluorescence intensity immediately after the dansyl-free vesicle addition, obtained by a linear extrapolation of the trace 3−4 min after the vesicle addition. The calculation of the extent of translocation is described elsewhere (Matsuzaki et al., 1996b). The true percent leakage value of calcein was employed as a measure of the pore formation. The peptide permeation (the circles in Figure 3) was almost coupled with the pore formation, suggesting that the pore formation−translocation is the mechanism of the membrane permeabilization by T-SS.

Mechanism of T-Acm Action in PG/PC Bilayers. Figure 2B clearly depicts that T-Acm failed to translocate under conditions (L/P = 100) comparable with those in Figure 2A. Figure 4A shows the dye efflux induced by the linear peptide. T-Acm 1 order of magnitude less effectively impaired the membrane barrier; the leakage was observed only at L/P ≤ 10. To clarify the mechanism, we determined the 90° light scattering intensity at 400 nm which is summarized in Figure 4B as values relative to the control without the peptide. At L/P = 50 where no dye efflux was observed, the scattering intensity was not changed by the peptide (trace 1). In contrast, with leakage-occurring L/P = 10, the intensity first increased and subsequently decreased to below unity, suggesting morphological changes in the vesicles, aggregation/fusion followed by micellization (Matsuzaki et al., 1993a,b). On the other hand, T-SS caused no change in light scattering at L/P = 100 where significant leakage was observed [data not shown; see also Matsuzaki et al. (1993a)].

Interaction with PG/PE Liposomes. Lipid composition can significantly modulate the peptide−lipid interactions. We also examined the effects of the peptides on the barrier property and the integrity of PG/PE (1/1) liposomes mimicking bacterial cell membranes. Figure 5A compares the calcein leakage induced by T-SS and T-Acm. T-SS triggered ca. 60% leakage during a 5-min incubation at L/P = 27 (trace 1). The PG/PE membrane was more resistant to the peptide-induced membrane permeabilization compared with the PG/PC bilayers where a similar extent of leakage was observed at a 4 times larger L/P value of 116 (Figure 3). The linear analog was again much weaker in lytic activity than T-SS. T-Acm induced only 20% leakage for 5 min at L/P = 8.5. A lower L/P value of about 3 was needed to cause a comparable extent of dye efflux in the case of PG/PC (Figure 4A), indicating that the PG/PE membrane is more susceptible to T-Acm, in striking contrast to T-SS.

Figure 5B depicts the relative light scattering intensity of the peptide-treated vesicles. The addition of each peptide to the liposomes resulted in a drastic change in intensity, i.e., an initial rise and a subsequent reduction below unity.

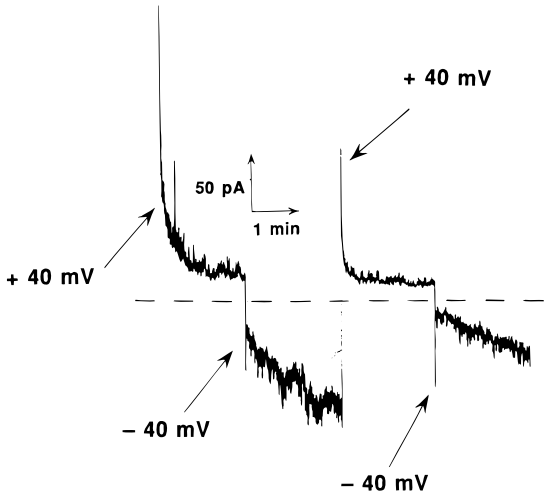

FIGURE 6: Polarity dependence of macroscopic current fluctuations induced by asymmetrically added T-SS. T-SS (3.3 μM) was added to the *cis* compartment with stirring. The current across PG/PE (1/1) planar bilayers was recorded under the voltage-clamped conditions indicated in the figure. The voltage is that of the *cis* relative to the *trans* compartment. The composition of the bathing solutions in both compartments was 100 mM KCl/10 mM Tris-Hepes (pH 7.4). Zero current level is shown as a dashed line.

The reduction in the presence of T-Acm (trace 2) was greater than that by T-SS (trace 1) in spite of the larger leakage induced by the latter peptide (Figure 5A).

Membrane Conductance Change. We compared the probability of detecting membrane current fluctuations in PG/PE (1/1) planar bilayers between the two peptides. We used the fraction of the number of runs in which membrane current fluctuations were observed within 30 min after the addition of each peptide to the *cis* compartment. T-SS (3.3 μM) exhibited membrane currents in 11 experiments out of 24 runs. In the other 13 experiments, the membrane was ruptured. In contrast, T-Acm showed no current up to a much higher concentration of 31.3 μM ($n = 8$).

Figure 6 depicts the effect of the voltage polarity on the membrane current triggered by T-SS (*cis*, 3.3 μM). By the constant application of a *cis*-positive potential of 40 mV, the current was decreased to ~20 pA (0.5 nS) within 1 min after a large instantaneous current. When the potential was switched to the *cis*-negative potential of −40 mV, the current was inverted to the same absolute current level with opposite direction, and then it was gradually increased to ca. 90 pA (2.2 nS). The plateau current reached by the constant potential application was larger at the negative potential than at the positive potential. The repeated application of the positive−negative cycle induced similar behavior of the current change. However, the magnitude of the current change, especially at the negative potential, was decreased, diminishing the current asymmetry. Figure 7 shows that the current was almost symmetrical when the peptide was present in both compartments (1.7 μM each).

The T-SS ion channel formation was occasionally observed at lower peptide concentrations (Figure 8). The main conductance was about 90 pS, although many other conductance levels (*e.g.*, 140, 210 pS) were also less frequently observed. The probability of the channel appearance was larger at a positive membrane potential of 57.6 mV than at a negative membrane potential of −58.5 mV (Figure 8A).

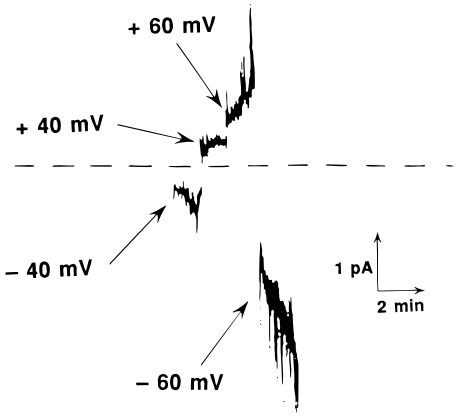

FIGURE 7: Polarity dependence of current fluctuations induced by symmetrical application of T-SS. The bilayer was formed with PG/PE (1/1) in 100 mM KCl/10 mM Tris-Hepes (pH 7.4). T-SS (1.7 μM) was added to both *cis* and *trans* compartments. Zero current level is shown as a dashed line.

Table 1 summarizes the Cl-to-K ion permeability ratios obtained from four independent experiments. The tachyplesin pore was found to be anion selective.

DISCUSSION

T-SS exhibited stronger membrane-permeabilizing abilities than T-Acm irrespective of the lipid composition (PG/PC versus PG/PE) and the membrane system (vesicles versus planar bilayers), in keeping with the more potent antimicrobial activity of the former peptide. The action mechanisms, however, are not the same, because both peptides respond differently to the lipid composition. The substitution of PE for PC reduces the activity of T-SS, whereas it enhanced the T-Acm potency.

Action Mechanism of T-SS. The cyclic peptide forms a calcein-permeable pore in the PG/PC membranes with the vesicle morphology intact. The peptide also translocates across the bilayer coupled with the pore formation (Figure 3). In our previous studies (Matsuzaki et al., 1995a,b, 1996b), we also employed other techniques for detecting the translocation, i.e., the trypsin digestion method and the NBD-dithionite assay. Unfortunately, both approaches did not work in the T-SS system. The enzyme failed to digest the cyclic peptide in the presence of liposomes. The reducing agent partially inactivates the peptide by cleaving the disulfide bonds.

The leakage activity of T-SS against the PG/PE liposomes was 4 times weaker than that against the PG/PC membranes. Furthermore, morphological changes of the vesicles accompanied the membrane permeabilization (Figure 5). The pore formation−peptide translocation mechanism also appears to operate in the PG/PE system; T-Acm induced a greater reduction in light scattering intensity in spite of a weaker leakage (Figure 5). The repeated application of the transmembrane potential of altering polarity decreased the asymmetry of the T-SS-triggered current (Figure 6), suggesting peptide translocation across the bilayer. The reason for the resistance of PG/PE is unclear at present. One possibility would be that the hydrogen-bonding ability of PE strengthens the peptide−lipid interactions, preventing the parallel-to-perpendicular change in the peptide orientation. Another possibility would be that if the peptide imposes a positive curvature on the membrane and the resultant

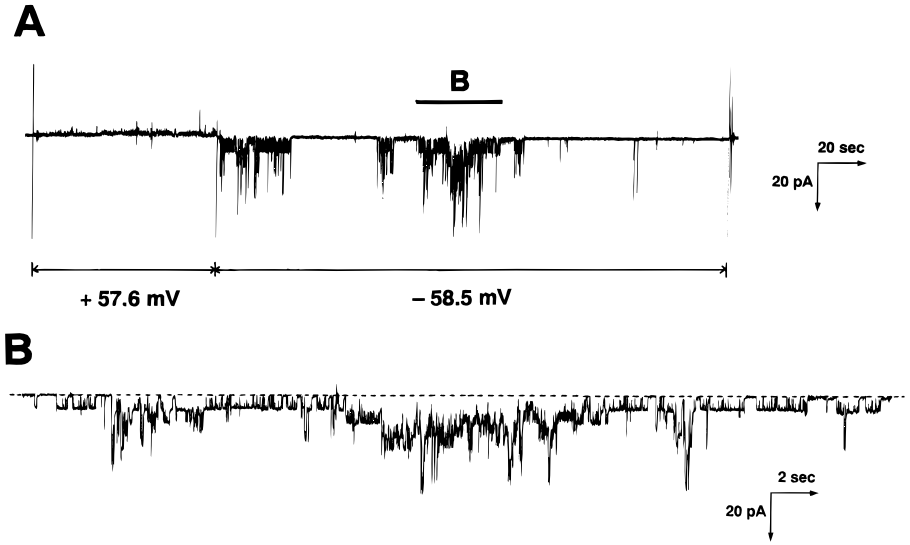

FIGURE 8: Current fluctuations induced by asymmetrically added T-SS at a low concentration. The bilayer was formed with PG/PE (1/1) in 100 mM KCl/10 mM Tris-Hepes (pH 7.4). (A) T-SS (2.3 μM) was added to the *cis* compartment under a voltage-clamped condition of −40 mV with stirring, and then the membrane potential was changed to the one indicated in the figure. (B) Expansion (10×) of the time scale of the current trace of A. The part expanded is shown as a bar and a letter B in the current trace of A. Zero current level is shown as a dashed line.

Table 1: Ion Selectivity of T-SS Channel

solution[a] (*cis*, *trans*)	run	reversal potential (mV)	P_{Cl}/P_K[b]
300, 100	1	16.42	4.18
	2	18.66	4.69
	3	21.50	8.58
500, 100	1	17.20	2.94

[a] The concentration of KCl in each compartment is shown in mM. [b] The Cl^- to K^+ permeability ratio was calculated from the reversal potential by use of the Goldman−Hodgkin−Katz equation (eq 2).

curvature modulation facilitates the pore formation−translocation, then PE could inhibit the process by inducing a negative curvature strain.

The planar bilayer experiments would provide more information on the property of the T-SS pore, although there is the possibility that the pore structure in the presence of the transmembrane potential somewhat differs from that in its absence. The cyclic peptide, T-SS, caused a macroscopic current change, which is dependent on the polarity of the membrane potential (Figure 6). Constant application of the *cis*-positive potential decreased the current, while the *cis*-negative potential increased it. At the point of switching the potential, the absolute value of the current was similar. This observation cannot be explained by an electrophoretic insertion of the positively charged peptide into the lipid matrix, because the *cis*-negative potential facilitated the current. This polarity dependence is opposite to that found in defensin NP-1, a β-sheet rich antimicrobial peptide (Kagan et al., 1990). Interestingly, the channel of polymyxin B, a basic cyclic antibiotic, also exhibits a *cis*-negative potential activation (Schröder et al., 1992). Symmetrical application of T-SS from both sides (*cis* and *trans*) of the planar bilayer increased the current at both positive and negative potentials (Figure 7), indicating that the asymmetry of the current change originates from the asymmetry of the peptide distribution.

The current fluctuation induced by the peptide is highly dependent on the peptide concentration. At the lower peptide concentration, T-SS forms ion channels with multiple conductance levels (Figure 8). The appearance of the ion channels is remarkable when the membrane potential is negative. This is consistent with the behavior of the macroscopic current.

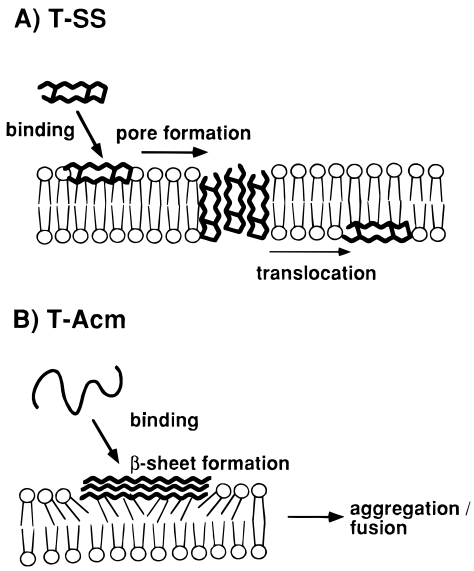

FIGURE 9: Models of tachyplesin−lipid bilayer interactions. (A) T-SS assumes a cyclic antiparallel β-sheet structure in both the aqueous and membranous environments because of the two intramolecular S−S linkages. The peptide binds to negatively charged lipid bilayers without significantly perturbing the membrane structure. Several peptide molecules self-aggregate to form anion-selective pores of various sizes. Upon their disintegration, a fraction of the peptides translocates into the inner leaflets. (B) T-Acm takes unordered structures in the solution. The peptide associates to acidic lipids forming an intermolecularly hydrogen-bonded β-sheet, which significantly destabilizes the bilayer organization. The liposomes finally aggregate and fuse.

On the basis of these observations, we would tentatively assume the following model (Figure 9A). T-SS assumes a cyclic antiparallel β-sheet structure in both the aqueous and membranous environments. The peptide binds to negatively charged lipid bilayers without significantly perturbing the membrane structure. A small portion of the peptide mol-

Table 2: Estimation of Pore Lifetime of T-SS

[peptide] (μM)	run	% leakage (apparent)	$Q_{observed}$	Q_{theory}[a] $\rho = 0.3$	Q_{theory}[a] $\rho = 0.4$
0.3	1	60.5	0.207	0.189	0.213
	2	60.4	0.211	0.189	0.213
0.5	1	82.3	0.276	0.258	0.303
	2	82.2	0.273	0.258	0.302

[a] Calculated according to Schwarz and Arbuzova (1995).

ecules self-aggregates to form anion-selective pores of various sizes. The ability of the pore to pass the ionic molecules is largely dependent on the membrane potential probably due to the conformational change in the T-SS peptide. The number of pores decreases with time because of the translocation of the peptide to the *trans* side of the bilayer.

The T-SS pore is anion-selective, as expected from the peptide's positive charges. Basic peptides sometimes show cation selectivity (Anzai et al., 1991; Cruciani et al., 1992). In the case of magainin 2, this apparent abnormal behavior was explained by the involvement of anionic lipids in the pore lining (Cruciani et al., 1992; Matsuzaki et al., 1996a). The T-SS pore may not contain a sufficient number of anionic lipids for the ion selectivity reversal.

Pore Lifetime and Translocation. To calculate the true percent leakage value from the observed apparent leakage value, the mode of leakage or the lifetime of the pore should be determined (Weinstein et al., 1984). If the lifetime, τ, is much longer than the intrinsic lifetime, τ_0, which is the time necessary for a $1/e$ reduction of the intravesicular dye concentration, then a single pore opening is sufficient to exhaust the vesicular contents ("all-or-none mode"). On the other hand, a number of pore openings are necessary to observe a significant extent of leakage in the case of $\tau << \tau_0$ ("graded mode"). In the latter mode, fluorescence from intravesicular diluted calcein should make a nontrivial contribution to the measured fluorescence. There are, of course, many cases between the above two extremes. Schwarz introduced the dimensionless parameter, ρ (Schwarz & Robert, 1992; Schwarz & Arbuzova, 1995):

$$\rho = \tau_0/(\tau_0 + \tau) \quad (3)$$

The all-or-none and the graded modes correspond to $\rho = 0$ and 1, respectively. The ρ value can be estimated by determination of the self-quenching factor, Q, of the intravesicular dye after the peptide treatment. After incubation of egg PC/egg PG (1/1) LUVs with the peptide for 10 min, the vesicle fraction was separated from leaked calcein by gel filtration, and its fluorescence intensity before (F_b) and after (F_a) addition of Triton X-100 was measured. The Q value is defined by F_b/F_a. Table 2 summarizes the results. The comparison of the determined Q values with the theoretical predictions (Schwarz & Arbuzova, 1995) evaluates the ρ value to be 0.3−0.4, which corresponds to $\tau \approx 2\tau_0 \approx 20$ ms (Matsuzaki et al., 1995b). Thus, we converted the apparent leakage to the true percent leakage (the curve in Figure 3), assuming $\rho = 0.35$. Figure 3 depicts the coupling between the pore formation and the peptide translocation. For example, 50% leakage corresponds to 27% translocation: about 200 tachyplesin molecules per vesicle are internalized. According to Schwarz's theory (Schwarz & Arbuzova, 1995), the number of pores, p, which had been formed can be expressed as

$$p = -\{\ln(1 - L)\}/(1 - \rho) \quad (4)$$

The extent of leakage is denoted by L ($0 \leq L \leq 1$). Therefore, the p value at $L = 0.5$ is estimated to be only ca. 1 in the case of $\rho = 0.35$: a single pore mediates the internalization of 200 peptides. This apparent peculiarity can be explained as follows. Figure 8 shows that the tachyplesin pore has various sizes. As judged from its conductance (90 pS), the diameter of the most frequently observed smallest channel is calculated to be approximately 0.5 nm, assuming that the pore is a cylinder filled with the electrolyte solution and that there is no specific interaction between the ions and the pore (Sansom, 1991). The size is smaller than that of the calcein dye (ca. 1 nm). Thus, most peptide molecules translocate across the bilayer through the calcein-impermeable pore.

Action Mechanism of T-Acm. Figure 9B schematically describes the action mechanism of T-Acm. Our previous FTIR−PATR study (Matsuzaki et al., 1993b) revealed that the linear peptide forms an interchain hydrogen-bonded β-sheet structure, significantly disturbing the bilayer organization. Such a large structure, which is not optimum for spanning the bilayer, fails to translocate across the membrane (Figure 2B), although its membrane binding is as strong as the affinity of T-SS (Matsuzaki et al., 1993b). T-Acm impairs the membrane barrier by destabilizing the membrane architecture with the morphological changes in the vesicles. In addition to the disorder of the acyl chain region (Matsuzaki et al., 1993b), the charge neutralization of the vesicle surface at lower L/P ratios would also contribute to the destabilization. The presence of fusion-promoting PE facilitates the permeabilization. The planar bilayer system devoid of interbilayer and intermonolayer interactions is more resistant to the T-Acm induced membrane lesion. In closed vesicles, any imbalance between the two leaflets would result in liposomal disintegration.

In summary, the disulfide bonds endow the tachyplesin peptide with the highly efficient mechanism for membrane permeabilization without significantly disrupting the vesicle organization, i.e., the anion-selective pore formation followed by translocation. We observed similar phenomena for helix-forming peptides, magainin 2 (Matsuzaki et al., 1995a,b) and mastoparan X (Matsuzaki et al., 1996b). Amphiphilic secondary structures capable of spanning the lipid bilayer (ca. 3 nm length) seem to be a structural motif necessary for the translocation.

REFERENCES

Akaji, K., Fujii, N., Tokunaga, F., Miyata, T., Iwanaga, S., & Yajima, H. (1989) *Chem. Pharm. Bull. 37*, 2661−2664.

Anzai, K., Hamasuna, M., Kadono, H., Lee, S., Aoyagi, H., & Kirino, Y. (1991) *Biochim. Biophys. Acta 1064*, 256−266.

Bartlett, G. R. (1959) *J. Biol. Chem. 234*, 466−468.

Bechinger, B., Kim, Y., Chirlian, L. E., Gesell, J., Neumann, J.-M., Montal, M., Tomich, J., Zasloff, M., & Opella, S. J. (1991) *J. Biomol. NMR 1*, 167−173.

Cruciani, R. C., Barker, J. L., Durell, S. R., Raghunathan, G., Guy, H. R., Zasloff, M., & Stanley, E. F. (1992) *Eur. J. Pharmacol.-Mol. Pharmacol. Sect. 226*, 287−296.

Fujita, K., Kimura, S., & Imanishi, Y. (1994) *Biochim. Biophys. Acta 1195*, 157−163.
Fujiwara, C., Anzai, K., Kirino, Y., Nagao, S., Nozawa, Y., & Takahashi, M. (1988) *J. Biochem. 104*, 344−348.
Kagan, B. L., Selsted, M. E., Ganz, T., & Lehrer, R. I. (1990) *Proc. Natl. Acad. Sci. U.S.A. 87*, 210−214.
Kawano, K., Yoneya, T., Miyata, T., Yoshikawa, K., Tokunaga, F., Terada, Y., & Iwanaga, S. (1990) *J. Biol. Chem. 265*, 15365−15367.
Matsuzaki, K., Fukui, M., Fujii, N., & Miyajima, K. (1991) *Biochim. Biophys. Acta 1070*, 259−264.
Matsuzaki, K., Fukui, M., Fujii, N., & Miyajima, K. (1993a) *Colloid Polym. Sci. 271*, 901−908.
Matsuzaki, K., Nakayama, M., Fukui, M., Otaka, A., Funakoshi, S., Fujii, N., Bessho, K., & Miyajima, K. (1993b) *Biochemistry 32*, 11704−11710.
Matsuzaki, K., Murase, O., Tokuda, H., Funakoshi, S., Fujii, N., & Miyajima, K. (1994) *Biochemistry 33*, 3342−3349.
Matsuzaki, K., Murase, O., Fujii, N., & Miyajima, K. (1995a) *Biochemistry 34*, 6521−6526.
Matsuzaki, K., Murase, O., & Miyajima, K. (1995b) *Biochemistry 34*, 12553−12559.
Matsuzaki, K., Murase, O., Fujii, N., & Miyajima, K. (1996a) *Biochemistry 35*, 11361−11368.
Matsuzaki, K., Yoneyama, S., Murase, O., & Miyajima, K. (1996b) *Biochemistry 35*, 8450−8456.
Montal, M., & Mueller, P. (1972) *Proc. Natl. Acad. Sci. U.S.A. 69*, 3561−3566.
Nakamura, T., Furunaka, H., Miyata, T., Tokunaga, F., Muta, T., Iwanaga, S., Niwa, M., Takao, T., & Shimonishi, Y. (1988) *J. Biol. Chem. 263*, 16709−16712.
Ohta, M., Ito, H., Masuda, K., Tanaka, S., Arakawa, Y., Wacharotayankun, R., & Kato, N. (1992) *Antimicrob. Agents Chemother. 36*, 1460−1465.
Sansom, M. S. P. (1991) *Prog. Biophys. Mol. Biol. 55*, 139−235.
Schröder, G., Brandenburg, K., & Seydel, U. (1992) *Biochemistry 31*, 631−638.
Schwarz, G., & Robert, C. H. (1992) *Biophys. Chem. 42*, 291−296.
Schwarz, G., & Arbuzova, A. (1995) *Biochim. Biophys. Acta 1239*, 51−57.
Takagi, M., Azuma, K., & Kishimoto, U. (1965) *Annu. Rep. Biol. Works Fac. Sci. Osaka Univ. 13*, 107−110.
Tamamura, H., Ikoma, R., Niwa, M., Funakoshi, S., Murakami, T., & Fujii, N. (1993a) *Chem. Pharm. Bull. 41*, 978−980.
Tamamura, H., Kuroda, M., Masuda, M., Otaka, A., Funakoshi, S., Nakashima, H., Yamamoto, N., Waki, M., Matsumoto, A., Lancelin, J. M., Kohda, D., Tate, S., Inagaki, F., & Fujii, N. (1993b) *Biochim. Biophys. Acta 1163*, 209−216.
Weinstein, J. N., Ralston, E., Leserman, L. D., Klausner, R. D., Dragsten, P., Henkart, P., & Blumenthal, R. (1984) In *Liposome Technology* (Gregoriadis, G., Ed.) pp 183−204, CRC Press, Boca Raton, FL.

BI970588V